

## Capillary Microflows in Porous Metals

Xuting Yang<sup>1</sup>, Yue Yang<sup>1</sup> and Yonggang Zhu<sup>1,2\*</sup>

<sup>1</sup>School of Mechanical Engineering and Automation  
Harbin Institute of Technology (Shenzhen), Shenzhen, Guangdong 518055, China

<sup>2</sup>School of Science, RMIT University, Melbourne, VIC 3001, Australia

### Abstract

Capillary flow in the porous media has received a lot of attention due to the applications in many areas, such as oil recovery, irrigation in agriculture, heat pipes and microfluidic pumping. While there have been numerous models to describe the wicking flow behaviour in different porous materials, it received much less attention for open foam porous metals and the flow behaviour is less understood. This paper reports the recent studies on the wicking behaviour of microfluid in treated copper foams with open cell pore structure. We use two types of nano-coated foams as the wicking medium, one of them with a thickness of 2 mm (porosity 96%) and the other with 1 mm thickness (porosity 92%). We treated the surface of the foams to obtain nano-structures, which changed the surface to be super hydrophilic with a near zero contact angle. The wicking experiment show that the wicking in our foams has two stages, with the initial stage of saturated wicking and later the unsaturated wicking. The measured results of wicking heights are presented for the two different foams.

### 1. Introduction

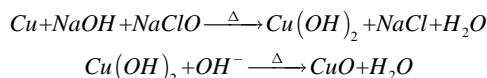
Capillary flow in porous media is a common phenomenon that often occurs in nature, e.g., rock soil and sand, and man-made forms, e.g., packed beads [6] and fabrics [3], ceramic [2], papers [4] and metal foams [10]. Flow of liquid or gas in porous media has received a lot of attention and widely used in many areas, such as oil recovery, irrigation in agriculture, heat pipes, and microfluidic pumping.

Open-cell metal foams have the properties of high porosity, low density, large surface area, good absorption and excellent physical and mechanical properties. Due to these advantages, metal foams have been widely used in two phase cooling devices for thermal management of electronics, such as flat heat pipes and heat spreaders. The liquid flows from the condensing end back to the evaporation end by the capillary action of the wicking material. The capillary limit of the heat transfer will be well solved if choosing the metal foams as the wicking material. Though the wicking performances in many types of porous media have been studied [2-4, 9], wicking in metal foams has not yet been fully characterized. There are many factors to influence the wicking performance in metal foams, such as the porosity, pore sizes, surface property, and permeability and so on. Fries and Dreyer considered the wicking in porous media under the influence of gravity, and derived an analytic solution for the capillary rise using the Lambert W function [1]. Shum et al. studied the effect of different compression factors on wicking ability of copper foams [10]. Shirazy et al. experimented with foam metal with different porosity and obtained corresponding permeability and influence on wicking ability [8]. From previous studies it is clear that there have been no appropriate models to describe capillary flows in porous metals. The aim of this study is to investigate the microflows in a porous metal with open cell pore structure with different thickness and provide experimental data for model development.

### 2. Experiment and Methods

#### 2.1 Material treatment

Two types of copper foams were used as the wicking medium, one of them with a thickness of 2 mm (porosity 96%) and the other with 1 mm thickness (porosity 92%), both were cut into rectangular with length ( $L$ ) of 100 mm, width ( $W$ ) of 15 mm. In order to achieve a high and stable wicking performance using copper foams, an oxidation process was used to create a super-hydrophilic surface on the foams [10], which means the contact angle  $\theta$  is close to 0. The principle of oxidation reaction is shown as follows,



The oxidation procedure includes the following steps. Firstly, the copper foams were cleaned in an ultrasonic bath with deionized water for five minutes and repeated for three times with fresh deionized water each time. Secondly, in the pickling process, the copper foams were cleaned with acetic acid (96 %) at 45 °C-50 °C for 60 minutes. Then the foams were cleaned with deionized water for 15 minutes and dried at 70 °C in the vacuum oven for 30 minutes. The oil stains and particles of the copper foams were removed effectively. The dried copper foams were placed into an alkaline solution at 90 °C for 30 minutes, which consisted of NaOH and NaClO<sub>2</sub> (2.1M) and had a strong oxidizing property. As shown in Fig. 1(a), the copper foams turned to black after the oxidation process because of the blacken nanostructures formed on the surface. Then the blacken foams were rinsed with deionized water for 15 minutes. Finally, the foams were dried again in the vacuum oven at 150 °C for 120 minutes. The nano-coated copper foams were used as the wicking material.

#### 2.2 Validation of contact angle and SEM images

The contact angle meter (KRUSS- DSA30) was used to check whether the contact angle turned to zero after oxidation process. The droplet for measurement was set as 4  $\mu\text{l}$ . The droplet was absorbed so fast that the absorption process cannot be taken within the limits of the instrument. The contact angle turns to zero in less than 15 ms as shown in figure 1-(b). After the oxidation process, the treated copper foams become super-hydrophilic. Nanostructured CuO (Copper oxide) surface was embellished with numerous nanowires growing on the ground and protuberances of micrometres, resulting in the contact angle near to zero. Figure 1-(c) shows the SEM images of original copper foams and nano-coated copper foams in different magnifications.

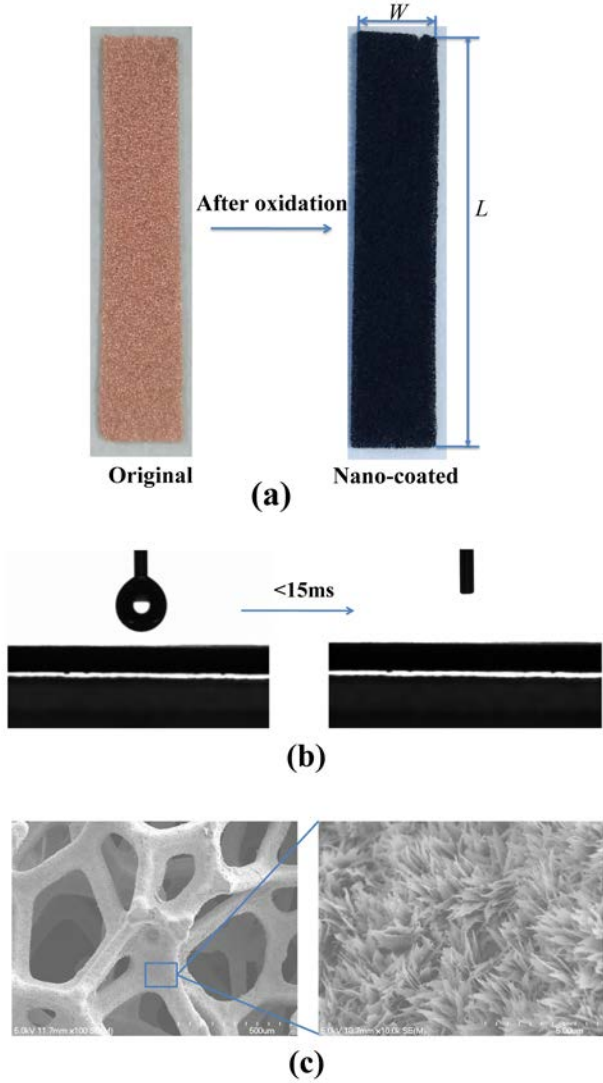


Figure 1. (a) Comparison of original copper foam and nano-coated copper foam. (b) The contact angle turns to zero in less than 15 ms on the surface of nano-coated copper foam. (c) SEM images of the treated copper foam at 250 x magnification about the structure of the pores and 10k x magnification about the nanostructures formed on the surface.

### 3. Theory

There have been numerous models to describe the wicking flow behaviour in different porous materials. One hundred years ago Lucas and Washburn [11] firstly studied the wicking in capillary. They concluded that the relation between the wicking height and the square root of time is linear when the gravity is neglected. They modelled the imbibition of liquid in porous media as the Hagen–Poiseuille [7] motion of liquid in a set of parallel capillary tubes behind a clear liquid front. While porous media have complex structures composed of numerous pores with different sizes, different shape and distributed freely, connected to each other, the flow in porous media is not parallel straight line, the classic Lucas Washburn equation cannot accurately describe the physics of wicking in porous media. Darcy [5] proposed a simple relation between the average liquid velocity and the pressure drop that has stood the test of time as a reliable and simple model for the flow of single liquids in porous media. The flow physics based on the Darcy's law was widely used. Fries and Dreyer considered the wicking in porous media under the influence of gravity, and derived an analytic solution for the capillary rise using the Lambert W function [1].

When wicking is performed in capillary tube, the momentum balance of a liquid inside gives:

$$\frac{2\sigma \cos \theta}{R} = \rho g h + \frac{8\mu h \dot{h}}{R^2} + \rho \frac{d(h\dot{h})}{dt} \quad (1)$$

Where  $\sigma$  is the surface tension,  $\theta$  is the contact angle,  $\mu$  is the dynamic viscosity,  $\rho$  is the density of the test liquid,  $R$  is the inner radius of tube,  $g$  is the gravity,  $h$  is the wicking height.

When it comes to wicking in porous media [1], the Darcy law can be used to describe the momentum balance:

$$\frac{2\sigma \cos \theta}{R_e} = \rho g h + \frac{\varphi \mu h \dot{h}}{K} + \rho \frac{d(h\dot{h})}{dt} \quad (2)$$

Where  $\varphi$  is the porosity of the porous medium,  $R_e$  is the effective pore radius of the porous medium,  $K$  is the permeability.

The analytic solution with the Lambert W function is as follows,

$$h(t) = \frac{a}{b} \left[ 1 + W \left( -e^{-1 - \frac{b^2 t}{a}} \right) \right] \quad (3)$$

Where  $a = \frac{2\sigma \cos \theta}{\varphi \mu} \frac{K}{R_e}$  and  $b = \frac{\rho K g}{\varphi \mu}$ .

Later the permeability  $K$  can be obtained by fitting the calculated liquid rise curve to experimental values [8].

The porosity of the porous media  $\varphi$  was calculated by the following equation,

$$\varphi = \left( 1 - \frac{V}{V_0} \right) \times 100\% \quad (4)$$

Where  $V$  is the solid volume of metal,  $V_0$  is the volume of the copper foam.

The liquid mass  $m$  is related to the wicking height according to the following equation [9],

$$m = \rho h W T \varphi \quad (5)$$

Where  $W$  is the width of the foam, and  $T$  is the thickness.

### 4. Wicking experiment set up

Wicking experiment was done at 25°C, standard atmospheric pressure. The deionized water was used as wicking liquid. The rate of wicking test was performed in two types of the nano-coated foams, and the thickness for one of them was 2 mm (porosity 96%) and another one was 1 mm (compressed from 2-mm-thick foam with the compression ratio 0.5, the corresponding porosity of 92%). Both foams were cut into rectangles with length of 100 mm, and width of 15 mm. Tests on each sample were repeated 3 times to obtain the objective data due to the variations of the measurement and foam microstructure. The experimental set-up used for the experiments is presented in Fig. 2. A CCD camera (Hamamatsu, Orca-spark) was used to catch the wicking front in the nano-coated foams at a minimum frame rate of 20 frames per second. The sample is suspended above the glass sink within the deionized water, which was controlled by a lab jack. The lab jack was used to move the liquid until touching the foam. As the water is colourless, the contrast between wetted and dry part was so small that is difficult to identify the wicking front, a bright light was added to the system to enhance the contrast, which makes the analysis of images much easier.

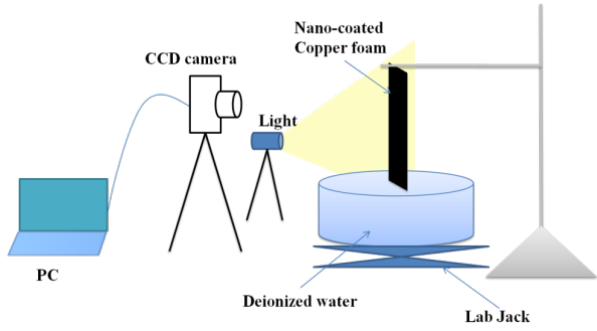


Figure 2. Experimental setup used for wicking experiments.

## 5. Results

Figure 3 shows the pictures of wicking phenomenon during experiments for the two pieces of metal foams. When the liquid touches the bottom of the nano-coated copper foam, wicking occurs quickly and reaches a saturated state in a short time. While the saturation state is maintained almost at a constant height, the liquid continues to wick in the vertical upward direction and forms an unsaturated wicking zone. Figure 3 also shows that the compressed foam (right images) has a higher wicking rate due to the smaller pores.

The measured wicking height as a function of time is shown in Fig. 4 for the two metal foams used. The result shows that the saturated equilibrium height (about 14 mm) is achieved in less than 1 s in the 2-mm-thick foam, the saturated equilibrium height (about 49 mm) is achieved in 10 s in the 1-mm-thick foam. The mass of water contained in the saturated area is  $4.03 \times 10^{-4}$  kg and  $6.62 \times 10^{-4}$  kg, calculated by the equation (5) respectively. After the saturation stage, the liquid fronts continued to move, albeit at a much slower rate. The maximum heights obtained for the observation time are 79 mm and 40 mm for the 1mm and 2 mm foams, respectively.

In this article, we focus on the saturated part. As the ratio  $K/R_e$  is a measure of pumping capacity of the wicking material [8], we fitted Eq. 3 to the experimental data of the saturated part to obtain the permeability and effective pore radius. The fittings are shown in Fig. 5(a) for the 2-mm-thick foam and Fig. 5(b) for the 1-mm-thick foam. For the 2 mm foam, the fitting parameters are  $a = 4.1407 \times 10^{-4}$ ,  $b = 0.0292$ , with the residual  $4.24 \times 10^{-6}$ . For the 1 mm foam, the fitting parameters are  $a = 4.505 \times 10^{-4}$ ,  $b = 0.0089$ , with the residual  $4.0232 \times 10^{-6}$ . From the fitting coefficients, we obtain the permeability  $K$  to be  $2.48 \times 10^{-9} \text{ m}^2$ ,  $R_e = 1010 \text{ } \mu\text{m}$  and  $7.29 \times 10^{-10} \text{ m}^2$ ,  $R_e = 285 \text{ } \mu\text{m}$  for the 1 mm and 2 mm foams, respectively. The ratio  $K/R_e$  is  $2.48 \times 10^{-6}$  for the 2 mm foam and  $3.12 \times 10^{-6}$  for the 1 mm foam.

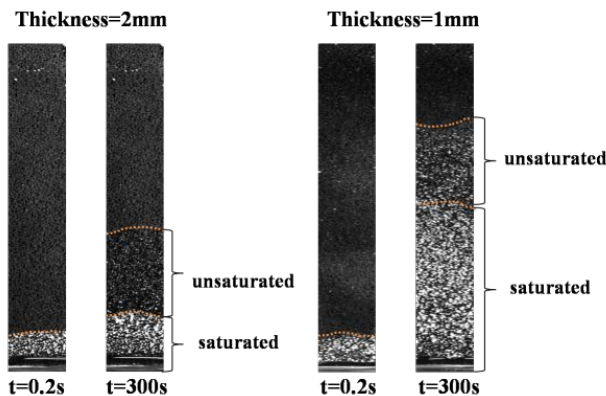


Figure 3. Pictures of liquid wicking of the two pieces of copper foams. Left: 2 mm thick foam, right: 1 mm thick foam.

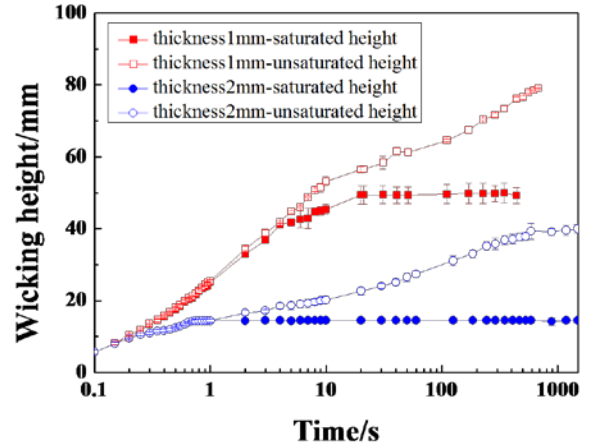


Figure 4. Wicking height as a function of time for the two metal foams. Blue circle symbols: 2 mm thick copper foam, Red square symbols: 1mm thick copper foam. Open symbols: overall wicking, closed symbols: only saturated.

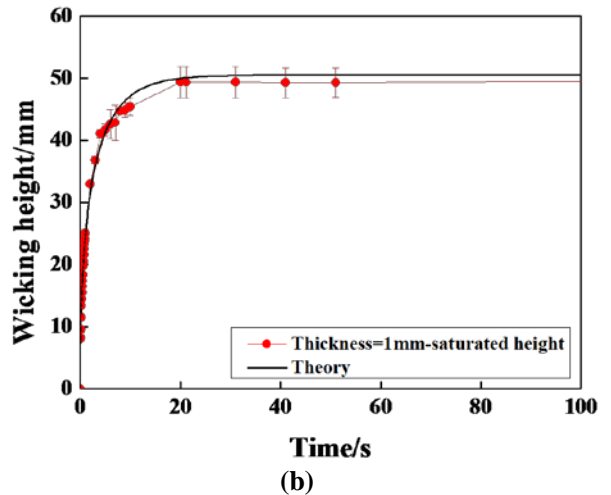
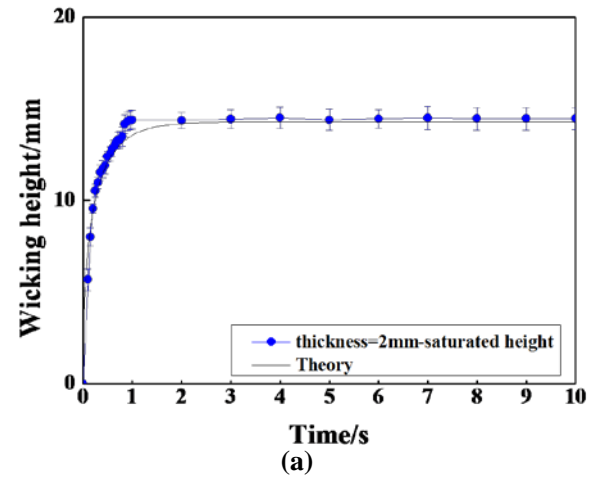


Figure 5. (a) Fitting the Eq. 2 to the experimental data about the foam with 2mm thickness under saturated conditions. (b) Fitting the Eq. 2 to the experimental data about the foam with 1mm thickness under saturated conditions

## 6. Conclusion

The behaviour of wicking microflows in porous metals have been investigated. The surface of the metal foams has been treated to obtain the super-hydrophilic layer of nanostructured CuO. The characteristics of the nanostructure have been examined by the SEM images. The wicking experiments reveals that there are two stages of wicking for the current two metal foams used, i.e. the initial stage of saturated wicking due to the inertial effect and the subsequent stage of slower unsaturated wicking. For the compressed foam with the thickness of 1mm, there is a 250% increase in wicking height both for the saturated and unsaturated stages.

## Acknowledgements

The financial supports from Harbin Institute of Technology and Shenzhen Science and Technology Innovation Commission for Prof. Yonggang Zhu are gratefully acknowledged. We thank Clifford Shum and Prof. Gary Rosengarten for providing the compressed copper foams.

## Reference

- [1] Fries, N. and M. Dreyer, An analytic solution of capillary rise restrained by gravity. *J Colloid Interface Sci*, 2008. 320(1): p. 259-63.
- [2] Gorjan, L., A. Dakskobler, and T. Kosmac, Partial wick-debinding of low-pressure powder injection-moulded ceramic parts. *Journal of the European Ceramic Society*, 2010. 30(15): p. 3013-3021.
- [3] Hamdaoui, M. and S. Ben Nasrallah, Capillary rise kinetics on woven fabrics - Experimental and theoretical studies. *Indian Journal of Fibre & Textile Research*, 2015. 40(2): p. 150-156.
- [4] Hansson, J., et al., Synthetic microfluidic paper: high surface area and high porosity polymer micropillar arrays. *Lab on a Chip*, 2016. 16(2): p. 298-304.
- [5] Jacob B, *Dynamics of Fluids in Porous Media*. New York: Elsevier Science, 1972.
- [6] Masoodi, R., K.M. Pillai, and P.P. Varanasi, Darcy's law-based models for liquid absorption in polymer wicks. *Aiche Journal*, 2007. 53(11): p. 2769-2782.
- [7] Salvatore P.S. and R. Skalak, The History of Poiseuille's Law. *Annual Review of Fluid Mechanics*, 2003. 25(1): p. 1-20.
- [8] Shirazy, M.R.S. and L.G. Frechette, Investigation of Capillary Properties of Copper Metal Foams by the Rate of Rise Method in the Presence of Evaporation, in 2012 13th Ieee Intersociety Conference on Thermal and Thermomechanical Phenomena in Electronic Systems. 2012. p. 710-716.
- [9] Shirazy, M.R.S. and L.G. Frechette, Capillary and wetting properties of copper metal foams in the presence of evaporation and sintered walls. *International Journal of Heat and Mass Transfer*, 2013. 58(1-2): p. 282-291.
- [10] Shum, C., G. Rosengarten, and Y. Zhu, Enhancing wicking microflows in metallic foams. *Microfluidics & Nanofluidics*, 2017. 21(12): p. 177.
- [11] Washburn, E.W., The Dynamics of Capillary Flow. *Physical Review*, 1921. 17(3): p. 273-283.